EARTHQUAKE ENGINEERING AND STRUCTURAL DYNAMICS, VOL. 26, 989–1003 (1997)

BEHAVIOUR OF CONTINUOUS PIPELINE SUBJECT TO TRANSVERSE PGD

XUEJIE LIU† AND MICHAEL J. O'ROURKE‡*
Department of Civil Engineering Rensselaer Polytechnic Institute, Troy, NY 12180-3590, U.S.A

SUMMARY

The response of buried continuous pipeline to tranverse Permanent Ground Deformation (PGD) has been studied by a number of investigators over the past few years. Herein the numerical results by O'Rourke[1] (1988) and Suzuki *et al.*[2] as well as analytical results by O'Rourke[3] are compared. It is shown that the numerical results specifically the peak tensile strain induced in the pipeline for moderate to large widths of the PGD zone (width $\geqslant 30$ m) agree reasonably well, and compare favourably with existing simplified, closed form, analytical results. However, the peak compressive pipe strains differ as well tensile strains for small widths of the PGD zone (width $W \approx 10$ m). New numerical results are presented which clarify these differences. In addition, an improved analytical model is introduced. Using information from PGD case histories primarily from Japan, the improved analytical model is shown to match reasonably well with numerical results. © 1997 John Wiley & Sons, Ltd.

Earthquake Engng. Struct. Dyn., **26**, 989–1003 (1997)

No. of Figures: 15. No. of Tables: 2. No. of References: 8.

KEY WORDS: buried pipeline; permanent ground deformation; pipe strain; transverse PGD

INTRODUCTION

For the seismic analysis and design of buried pipelines, two separate hazards are typically considered. The wave propagation hazard refers to transient strains induced in a pipeline due to travelling wave effects. The Permanent Ground Deformation (PGD) hazard refers to pipeline strain due to landslides, ground settlement or liquefaction-induced lateral spreading.

In discussing the PGD hazard, one must distinguish between longitudinal PGD and transverse PGD. Longitudinal PGD refers soil movement parallel to the pipe axis while transverse PGD refers to soil movement perpendicular to the pipe axis. In general, any arbitrary ground deformation can be decomposed into a longitudinal and a transverse component. For continuous (e.g. welded steel) pipelines subject to longitudinal PGD, O'Rourke *et al.*[4] have developed relationships between pipe strain, the amount of ground movement, and the spatial extent of the PGD zone. Based on these relationships, O'Rourke and O'Rourke[5] correctly predicted the observed behaviour to six pipelines along Balboa Blvd., which were subject to longitudinal PGD during the 1994 Northridge earthquake. The analysis indicated that three Grade-B (GR-B) steel pipelines (two large diameter water pipelines with welded slip joints and one gas pipeline with unshielded electric arc joints) would fail while three butt welded gas pipelines would survive, which was, in fact, the observed behaviour. Hence existing models for buried pipe response to longitudinal PGD appear adequate. This paper focuses on pipe response to transverse PGD.

* Correspondence to: M. J. O'Rourke, Department of Civil Engineering, Rensselaer Polytechnic Institute, Troy, NY 12180-3590, U.S.A.
† Research Assistant
‡ Professor

Contract grant sponsor: NCEER

CCC 0098–8847/97/100989–15$17·50

Received 12 September 1996
Revised 28 January 1997

When subject to tranverse PGD, a continuous pipeline will stretch and bend as it attempts to accomodate the tranverse ground movement. The failure mode for the pipe depends then upon the relative amount of axial tension (stretching) and flexural (bending) strain. That is, if the axial tension strain is low, the pipe wall may buckle in compression due to excessive bending. On the other hand, if axial tension is not small, the pipe may rupture in tension due to the combined effects of axial tension and flexure.

Pipeline response to transverse PGD is, in general, a function of the amount of ground movement δ, the width W of the PGD zone, as well as the pattern of ground deformation. In this paper, continuous pipeline response to spatially distributed transverse PGD in which the ground movement towards the centre of the PGD zone is substantially larger than that close to the margins is discussed. Herein the pipeline is assumed to be contained in a competent soil layer which overrides a liquefied layer below when the PGD is due to lateral spreading. Various analytical idealizations of the spatial distribution (i.e. the pattern of ground deformation) for transverse PGD which have been used in the past are reviewed. Results from existing analytical and numerical model are compared and differences are noted. New numerical and analytical results are presented which clarify the differences. Finally, the new simplified, closed form, analytical approach proposed herein is shown to work reasonably well for combinations of ground movement δ and width W observed in case histories of transverse PGD in Japan.

IDEALIZATIONS OF SPATIALLY DISTRIBUTED TRANSVERSE PGD

One of the first items needed to evaluate pipeline response is the pattern of ground deformation, that is, the variation of ground displacement across the width of the PGD zone. Different researches have used different patterns in their analyses. O'Rourke[1] approximates the soil deformation with the beta probability density function.

Suzuki *et al.*[6] approximate the transverse soil deformation by a cosine function raised to a power n. O'Rourke[3] assumes the following analytical form for spatially distributed transverse PGD:

$$y(x) = \frac{\delta}{2}\left(1 - \cos\frac{2\pi x}{W}\right) \tag{1}$$

where x is the distance from the margin of the PGD zone. Equation (1) gives the same shape as the Suzuki *et al.* model with $n = 2{\cdot}0$.

As shown in Figure 1, all the patterns are similar in that the maximum soil deformation occurs at the centre of the PGD zone and the soil deformation at the margins is zero. The patterns differ in the variation of ground deformation between the centre and the margins.

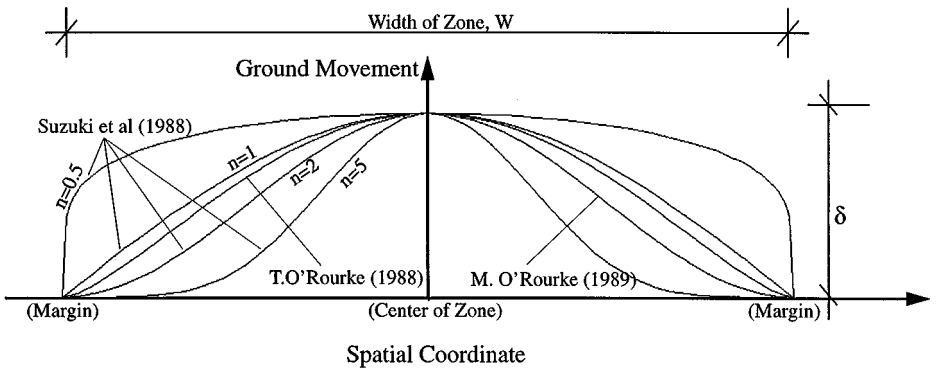

Figure 1. Assumed patterns for spatially distributed transverse PGD

PREVIOUS FINITE ELEMENT RESULTS

The finite element method allows explicit consideration of the non-linear characteristics at the pipe–soil interface in both the transverse and longitudinal directions as well as non-linear stress–strain relations for pipe material. O'Rourke[1] and Suzuki *et al.*[6] have used the finite element approach to evaluate buried pipe response to spatially distributed transverse PGD. Assumptions and numerical results from each are presented below.

T. O'Rourke[1]

O'Rourke[1] considered the physical model sketched in Figure 2.

As shown in Figure 2, L_a is the distance from the margin of the PGD zone to an assumed anchor point in the undisturbed soil beyond the PGD zone. The assumed anchor point in the O'Rourke[1] model was located where the pipe bending strain is less than 1×10^{-5}.

The O'Rourke[1] results for maximum tensile strain are shown in Figure 3 as a function of the maximum ground displacement for various widths of the PGD zone. Results in this figure are for X-60 grade pipe with diameter $D = 0{\cdot}61$ m, wall thickness $t = 0{\cdot}0095\,m$ and burial depth $H = 1{\cdot}5$ m. For the the three widths considered, the width of 10 m results in the largest tensile strain in the pipe for any given value of δ.

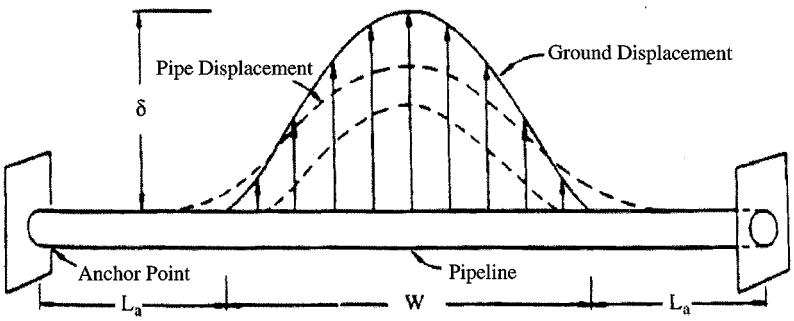

Figure 2. Physical model of pipeline and soil deformation (after T. O'Rourke)

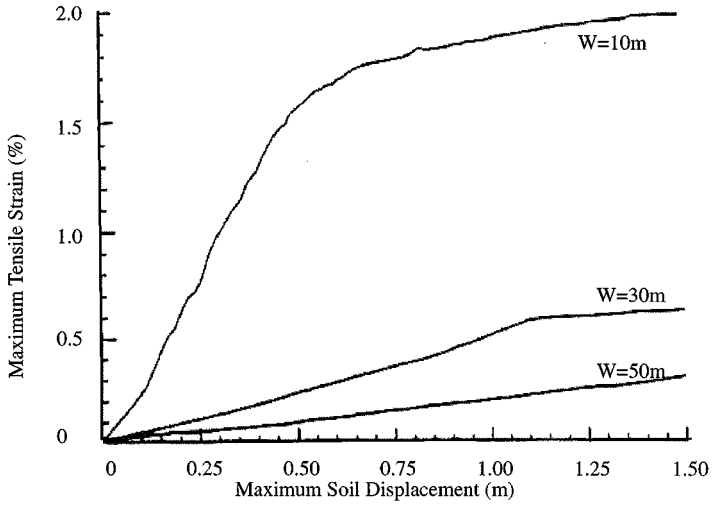

Figure 3. Maximum tensile strain vs. maximum ground displacement for three widths (after O'Rourke)[1]

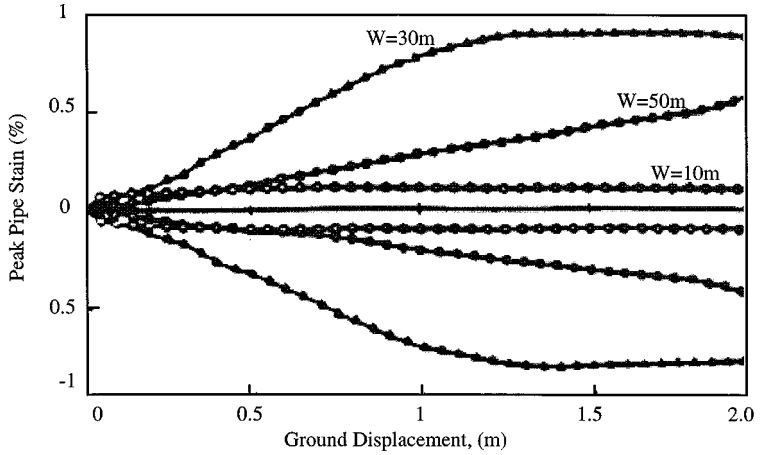

Figure 4. Maximum strain vs. PGD for $W = 10$, 30 and 50 m (after Suzuki *et al.*)

O'Rourke[1] also presents a plot of the maximum compressive strain as a function of δ for various values of the soil friction angle. Based on these results, O'Rourke[1] concluded that the width of the PGD zone has a greater influence on the magnitude of tensile strains than the soil properties.

For given values of the ground movement δ and the width of the PGD zone W, the pipe tensile strain is larger than the compressive strain. This suggests the induced axial strain in the pipe is significant. That is, if the axial strain was small, the peak tensile and compressive strains would be about equal.

Suzuki et al.[6]

Suzuki *et al.*[6] expressed the pattern of transverse ground displacements by the cosine function raised to the n power as shown in Figure 1. The patterns for $n \geqslant 1$ correspond to spatially distributed transverse PGD.

Suzuki *et al.*'s physical model is similar to O'Rourke's shown in Figure 2 except for the anchor length L_a. Suzuki *et al.* note that L_a needs to be long enough such that axial friction at the pipe–soil interface between the anchor points can fully accommodate the axial movement of the pipe due to PGD. That is, there should be no flexural or axial strains in the pipe at the anchor points. It turns out that the anchor length in Suzuki *et al.*'s model is much larger than that in the O'Rourke[1] model (small flexural pipe strain at the anchor point).

Figure 4 presents the Suzuki *et al.* pipe strain results for X-52 grade steel, $D = 0{\cdot}61$ m, $t = 0{\cdot}0127$ m and $H = 1{\cdot}5$ m. For given values of W and δ, the tensile and compressive strains are about equal. This suggests that the axial strain in the pipe is small. A certain width of the PGD zone some-where around 30 m results in the largest pipe strain. Note that although the pipes are somewhat different, the tensile pipe strains in Figures 3 and 4 are similar for $W = 30$ and 50 m.

RECENT FINITE ELEMENT RESULTS

By using the finite element computer program ABAQUS, the authors developed a finite element model, utilizing large deformation theory, non-linear pipe-soil interaction forces (soil springs) and Ramberg-Osgood stress–strain relations for the pipe material. The pipe is modelled as a beam coupled by both axial and lateral soil springs. The bases of soil springs outside of the PGD zone are fixed while the bases of the soil springs move with the soil. One hundred beam elements were used to model the pipeline over the width W of the PGD zone. The anchor length of the pipe is long enough (up to 400 m) such that both the flexural and axial pipe strain are essentially zero at the two anchor points. The pipe is assumed surrounded by loose to moderately dense sand (friction angle $\phi = 35^\circ$ and soil density $\gamma = 1{\cdot}87 \times 10^4$ N/m^3) with a burial depth

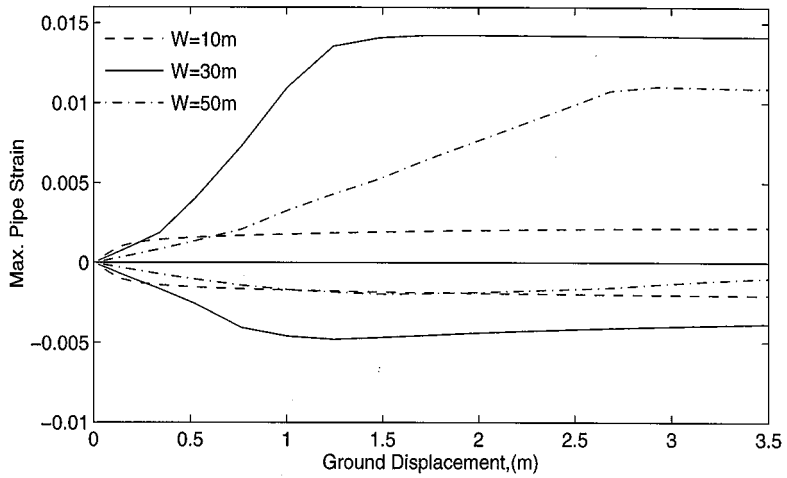

Figure 5. Maximum pipe strain vs. ground deformation

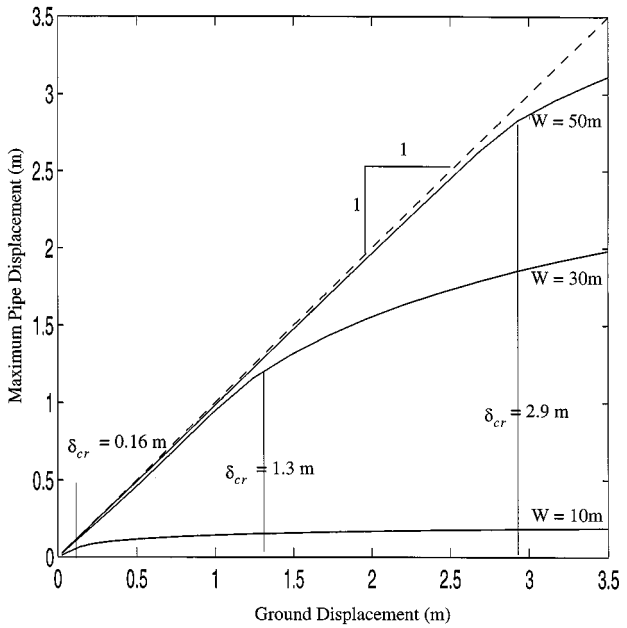

Figure 6. Maximum pipe displacement vs. ground displacement

$H_c = 1{\cdot}2$ m from ground surface to the top of the pipe. The resulting elastoplastic soil spring used herein are based U.S. Guideline[7] and have peak transverse, p_u, and longitudinal, t_u, resistance of $1{\cdot}0 \times 10^5$ and $2{\cdot}4 \times 10^4$ N/m, respectively. The relative displacements between pipe and soil at which the peak transverse and longitudinal soil resistances are mobilizing are 0·06 and $3{\cdot}8 \times 10^{-3}$ m, respectively.

Figure 5 shows the maximum tensile and compressive strains in the pipe versus the ground displacement for $W = 10, 30$ and 50 m, while Figure 6 shows the maximum pipe displacement versus the maximum ground displacement. Both these figures are for X-52 grade steel pipe with $D = 0{\cdot}61$ m, $t = 0{\cdot}0095$ m and the ground

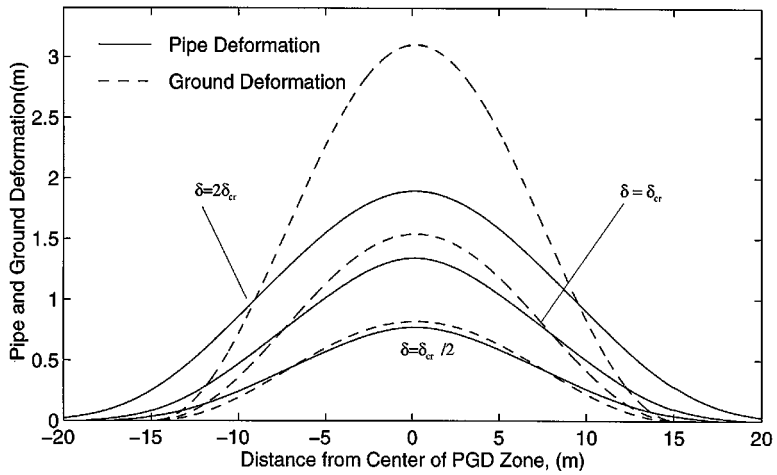

Figure 7. Pipe and ground deformation for $W = 30$ m

deformation pattern given in Equation (1). Except for $W = 10$ m, Figure 5 indicates that the peak tensile strain is substantially larger than the peak compressive strain, particularly for larger values of δ. Also for the three widths considered, the pipe strains are largest for $W = 30$ m. Although the pipes are somewhat different, the peak tensile strains shown in Figure 5 match reasonably well with Suzuki *et al.*'s shown in Figure 4 for all three widths. Also both the peak tensile and compressive strains match reasonably well with the O'Rourke[1] results for $W = 30$ and 50 m.

As shown in Figure 6, the maximum pipe displacement more or less matches the ground deformation up to a certain critical displacement δ_{cr}. Thereafter the pipe strain remains relatively constant while the pipe displacement increases more slowly with ground deformation. For ground deformation greater than δ_{cr}, the pipe bending strain varies slightly (increasing for small widths and decreasing for large widths) and axial strain increases slowly, which results in the maximum tensile remaining more or less constant.

For a fixed value of the width of the PGD zone ($W = 30$ m), Figure 7 shows the spatial distribution of pipe and soil displacement for $\delta = 0{\cdot}5\delta_{cr}$, δ_{cr} and $2\delta_{cr}$.

Note that the pipe deformation matches fairly well with the ground deformation over the whole width of the PGD zone for $\delta \leqslant \delta_{cr}$. However, for $\delta > \delta_{cr}$, the maximum displacement is less than the maximum ground displacement (from Figure 7, 40 percent less for $\delta = 2\delta_{cr}$), and 'width' of the deformed pipe (i.e. length over which the pipe has noticeable transverse displacement) is larger than the width of the PGD zone. As a result, the curvature of the pipe is substantially less than the curvature of the ground for $\delta > \delta_{cr}$. As shown in Figure 7 for $W = 30$ m, the pipe curvature at $\delta = 2\delta_{cr}$ is comparable to the pipe curvature at $\delta = \delta_{cr}$.

The transverse loading on the pipe also results in axial movement of the pipe, that is, inward movement towards the centre of the PGD zone. This inward movement is an increasing function of the ground movement δ. For $\delta = 4$ m, this inward movement at the margins of the PGD zone for the pipe under consideration was 0·002, 0·07 and 0·15 m, respectively, for $W = 10$, 30 and 50 m.

Figures 8 and 9 show the distribution of bending moment and axial forces in the pipe at $\delta = \delta_{cr}$ for $W = 10$, 30 and 50 m.

As one might expect, the bending moments in Figure 8 are symmetric with respect to the centre of the PGD zone and similar to those for a laterally loaded beam with built-in (i.e. fixed) supports near the margins of the PGD zone. That is, there is positive moment near the centre of the PGD zone and negative moments near the margins. The moments vanish roughly 10 m beyond the margins. Note that the bending moments for $W = 30$ m are larger than those for $W = 10$ m or 50 m.

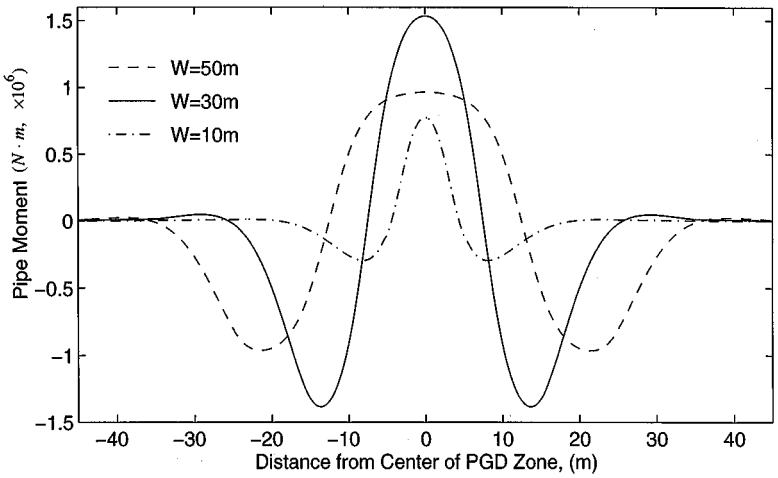

Figure 8. Distribution of bending moment for three widths ($\delta = \delta_{cr}$)

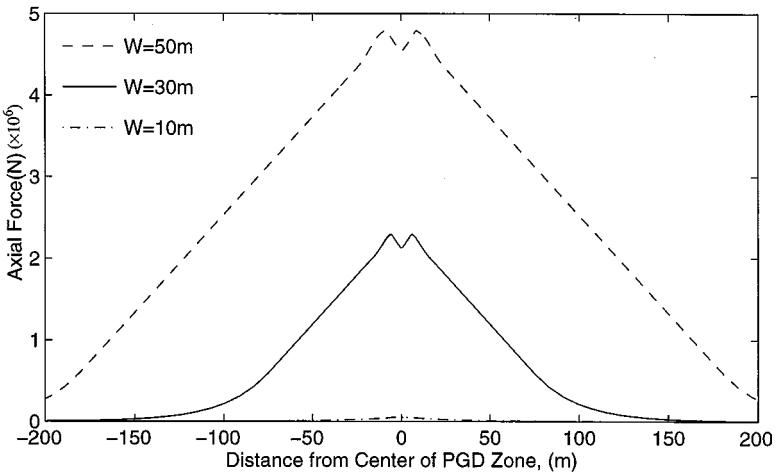

Figure 9. Distribution of axial force for three widths ($\delta = \delta_{cr}$)

The axial force in the pipe shown in Figure 9 is, as expected, also symmetric about the centre of the PGD zone. The axial force is maximum near the centre of the zone and decreases in a fairly linear fashion with increasing distance from the centre of the zone. Unlike the moments, the axial force becomes small only at substantial distances beyond the margins of the zone (note the different distance scales in Figures 8 and 9). Also, for the three widths considered, the axial force was an increasing function of the width of the PGD zone (i.e. largest for $W = 50\,\text{m}$ and smallest for $W = 10\,\text{m}$).

The influence of other parameters upon the pipe behavior was also determined and is shown in Figures 10–13. Unless otherwise indicated, these results are for $W = 30\,\text{m}$, X-52 grade steel, $D = 0{\cdot}61\,\text{m}$, $t = 0{\cdot}0095\,\text{m}$, $p_u = 1{\cdot}0 \times 10^5\,\text{N/m}$, $t_u = 2{\cdot}4 \times 10^4\,\text{N/m}$ and the O'Rourke[3] pattern of ground deformation. Figure 10 shows for example, the influence of diameter on peak tensile and compressive strains. Note that both the peak tensile and compressive strains are increasing functions of diameter.

For the pipe model considered the peak tensile strain is, to a greater or lesser extent, a function of all the parameters shown in Figures 10–13 as well as the steel grade and the anchor length L_a. However the peak

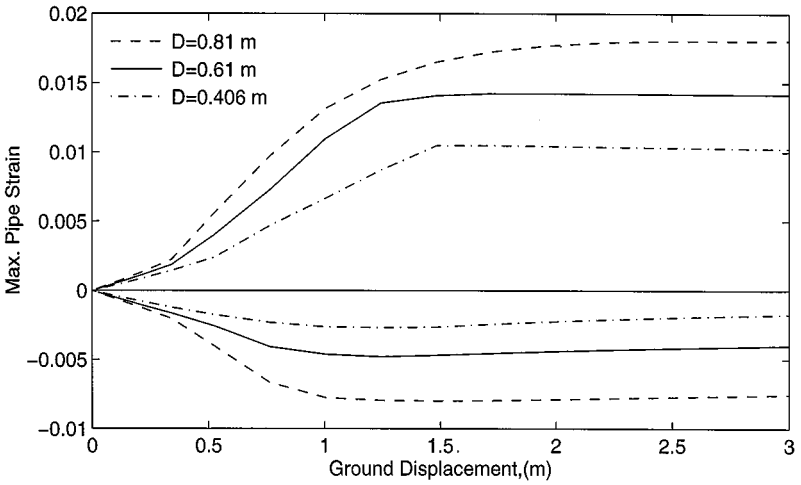

Figure 10. Influence of pipe diameter, D

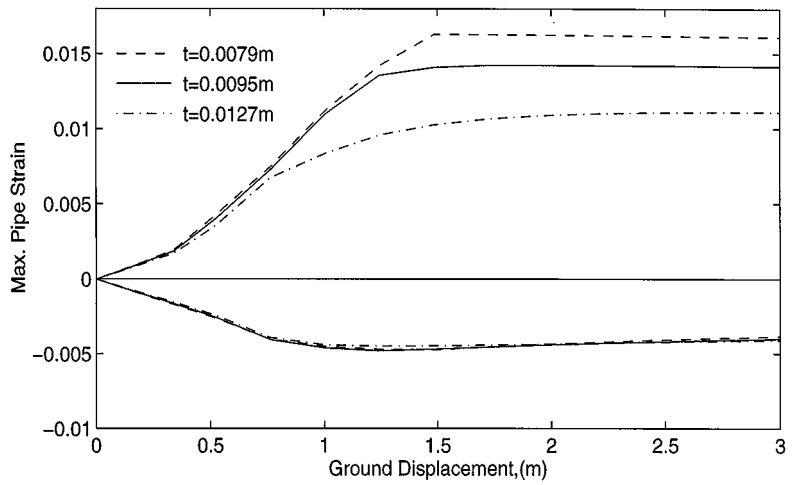

Figure 11. Influence of wall thickness, t

compressive stain is essentially independent of the wall thickness, as shown in Figure 11, and the steel grade.

The peak tensile strain in an increasing function of the pipe diameter and the transverse (lateral) soil spring resistance. It is a decreasing function of the pipe wall thickness, the steel grade and to a lesser extent the longitudinal (axial) soil spring resistance.

In terms of anchor length L_a, a zero anchor length resulted in substantially larger pipe strain than $L_a = 15\,\text{m}$ or 400 m. With reference to the PGD pattern, the O'Rourke[3] pattern (same as the Suzuki *et al.* pattern with $n = 2$) resulted in the largest pipe strain for $W \geqslant 30\,\text{m}$. However the Suzuki *et al.*[6] pattern with $n = 1$ resulted in the largest strain for $W \leqslant 10\,\text{m}$.

The parameter which most strongly influence the tensile strain is the width of the PGD zone, followed by the transverse soil spring resistance, pipe diameter, steel grade, wall thickness, PGD pattern, anchor length of

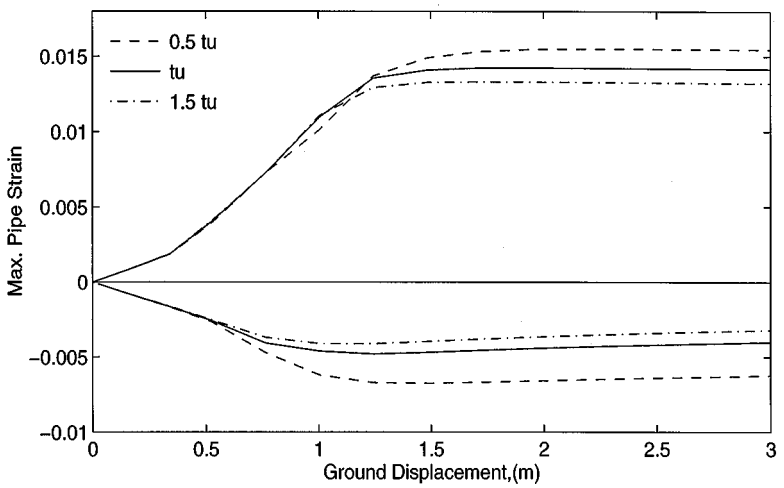

Figure 12. Influence of peak longitudinal soil resistance, t_u

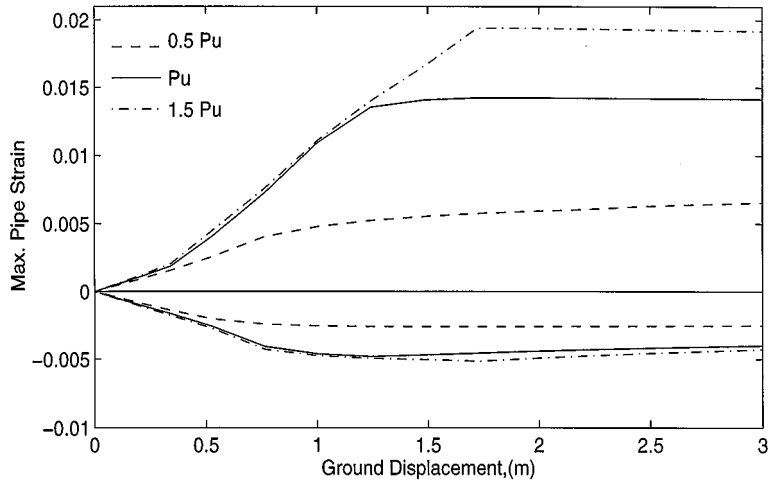

Figure 13. Influence of peak transverse soil resistance, p_u

the pipe and longitudinal soil spring resistance (skin friction). The critical ground displacement δ_{cr} was found to be an increasing function of width of the PGD zone and the lateral pipe–soil interaction force, but a decreasing function of steel grade, pipe diameter, axial pipe–soil interaction force and pipe wall thickness.

Based on these recent Finite Element results described above, it appears that axial effects are important in that the tensile strains are larger than the compressive strains. This agrees with previous numerical results by O'Rourke.[1] In addition, for the three widths considered, the tensile strains are largest for $W = 30$ m which agrees with previous numerical results by Suzuki *et al.*[6] However, the recent numerical results described above differ from those by O'Rourke,[1] specifically for the width of the PGD zone $W = 10$ m. Similarly the recent numerical results differ from those by Suzuki *et al.*[6] in that the tensile pipe strains are significant larger than the compressive strains. It is believed that this difference is due to the comparatively heavy wall thickness used in the Suzuki *et al.*[6] model (note as shown in Figure 11 that a heavier wall thickness reduces

the peak tensile strain but essentially has no effect on the peak compressive strain) in combination with a relatively weak longitudinal soil spring.

PREVIOUS ANALYTICAL APPROACH

O'Rourke[3] developed a simple analytical model for pipeline response to spatially distributed transverse PGD. He considered two types of response. For a wide width of the PGD zone, the pipeline is relatively flexible and its lateral displacement is assumed to closely match that of the soil. For this case the pipe strain was assumed to be mainly due to the ground curvature (i.e. displacement controlled). For a narrow width, the pipeline is relatively stiff and the pipe lateral displacement is substantially less than that of the soil. In this case, the pipe strain was assumed to be due to loading at the soil–pipe interface (i.e. loading controlled).

For the wide PGD width/flexible pipe case, the pipe is assumed to match the soil deformation given by Equation (1). The maximum bending strain, ε_b, in the pipe, is given by

$$\varepsilon_b = \pm \frac{\pi^2 \delta D}{W^2} \tag{2}$$

In this simple model, the axial tensile strain is based solely upon the arclength of the pipe between the PGD zone margins. Assuming the pipe matches exactly the lateral soil displacement, the average axial tensile strain, ε_a, is approximated by

$$\varepsilon_a = \left(\frac{\pi}{2}\right)^2 \left(\frac{\delta}{W}\right)^2 \tag{3}$$

For the narrow width/stiff pipe case, the pipe is modeled as a beam, built-in at each margin (i.e. fixed–fixed beam), subject to the maximum lateral force per unit length p_u at the soil–pipe interface. For this case the axial tension due to arclength effects is small and neglected. Hence, the maximum strain in the pipe is given by

$$\varepsilon_b = \pm \frac{p_u W^2}{3\pi E t D^2} \tag{4}$$

Note that O'Rourke[3] assumes that the pipe is fixed at the margins and hence neglects any inward (i.e. axial) movement of pipe at the margin of PGD zone. As a result, equation (3) overestimates the axial strain in the pipe, as will be shown later.

RECENT ANALYTICAL APPROACH

The recent Finite Element (FE) results suggest that pipe strain is an increasing function of ground displacement for ground displacement less than a certain value, δ_{cr}, and pipe strain does not change appreciably thereafter. For example, for $W = 30$ m, as shown in Figure 5, the maximum tensile strain is an increasing function of maximum soil displacement up to a value of $\delta = 1{\cdot}3$ m. For larger values of δ, the maximum tensile strain remains at a relatively constant value of roughly 0·014. Similar behaviour is observed for other widths.

In reality, the pipe resistance to transverse PGD is due to a combination of flexural stiffness and axial stiffness. The analytical relations developed below are for an elastic pipe. Although the inelastic pipe case is more complex, the elastic relations provide a basis for interpreting finite element results and, as will be shown later, are directly applicable to transverse PGD case histories from Niigata.

For small widths of the PGD zone, critical ground deformation and pipe behaviour are controlled by bending. The mechanism is the same as that in the O'Rourke[3] model for the stiff pipe case (i.e. two-end fixed

beam with constant distributed load). The critical ground deformation is given by

$$\delta_{\text{cr-bending}} = \frac{p_u W^4}{384EI} \tag{5}$$

For very larger widths of the PGD zone, the pipe behaves like a flexible cable (i.e. negligible flexural stiffness). For this case, the critical displacement is controlled primarily by the axial force. For parabolic cable, the relation between the axial force T at the ends and the maximum lateral deformation (or sag) δ is given by

$$T = \frac{p_u W^2}{8\delta} \tag{6}$$

As shown in Figure 7, the ground displacement is larger than the pipe displacement in the middle region of the PGD zone (assumed herein to be $W/2$), over which the maximum transverse resistance per unit length, p_u, at the pipe–soil interface (i.e. the distributed load) is imposed. Taking the 'sag' over this middle region to be $\delta/2$, the interrelationship between the tensile force, T, and ground displacement, δ, is given by

$$T = \pi Dt\sigma = \frac{p_u (W/2)^2}{8(\delta/2)} = \frac{p_u W^2}{16\delta} \tag{7}$$

where σ is the axial stress in the pipe (assumed to be constant within the PGD zone).

Inward movement of the pipe occurs at the margin of the PGD zone due to this axial force. Assuming a constant longitudinal friction force, t_u, beyond the margins, the pipe inward movement at each margin is

$$\Delta_{\text{inward}} = \frac{\pi Dt\sigma^2}{2Et_u} \tag{8}$$

The total axial elongation of the pipe within the PGD zone is approximated by the average axial strain given by equation (3) (i.e. arclength effect) times the width W. This elongation is due to stretching within the zone ($\sigma W/E$) and inward movement at the margins from equation (8):

$$\frac{\pi^2\delta^2}{4W} = \frac{\sigma W}{E} + 2\frac{\pi Dt\sigma^2}{2Et_u} \tag{9}$$

The critical ground deformation, $\delta_{\text{cr-axial}}$ for 'cable-like' behaviour and the corresponding axial pipe stress, σ, can be calculated by simultaneous solution of equations (7) and (9). These values are presented in Table I for three values of the width W and the standard properties mentioned previously (i.e. $D = 0.61$ m, $t = 0{\cdot}0095$ m, $p_u = 1{\cdot}0 \times 10^5$ N/m, $t_u = 2{\cdot}4 \times 10^4$ N/m). Note that the critical ground deformation is controlled by axial force for this case, and that the maximum axial stress at $\delta = \delta_{cr}$ in an increasing function of width of the PGD zone.

For any arbitrary width of the PGD zone, somewhat between small and very large, resistance is provided by both flexural (beam) and axial (cable) effects. Considering these elements to be acting in parallel,

$$\delta_{cr} = \frac{1}{\dfrac{1}{\delta_{\text{cr-bending}}} + \dfrac{1}{\delta_{\text{cr-axial}}}} \tag{10}$$

Table II lists the resulting critical displacements of an elastic pipe ($D = 0{\cdot}61$ m, $t = 0{\cdot}0095$ m, etc.) for $W = 10$, 30 and 50 m along with the corresponding elastic finite element results. For $W = 30$ and 50 m, the critical displacement from equation (10) matches that from the elastic finite element model. However, for $W = 10$ m, the critical displacement from equation (10) is an order of magnitude less than that from the elastic finite element model. This is due, in part, to the assumption of a constant transverse load p_u on the pipe for bending

Table I. Critical ground displacements and stresses for 'cable-like' elastic pipe

Item	$W = 10$ m	$W = 30$ m	$W = 50$ m
$\delta_{\text{cr-axial}}$ (equations (7) and (9))	0·37 m	1·5 m	2·85 m
σ (equations (7) and (9))	92·8 MPa	206 MPa	301 MPa

Table II. Critical ground displacements for elastic pipe

Item	$W = 10$ m	$W = 30$ m	$W = 50$ m
$\delta_{\text{cr-bending}}$ (equation (5))	0·015 m	1·22 m	9·6 m
$\delta_{\text{cr-axial}}$ (Table I)	0·37 m	1·5 m	2·85 m
δ_{cr} (equation (10))	0·015 m	0·67 m	2·2 m
δ_{cr} (FE Approach)	0·16 m	0·70 m	2·1 m

effects in the simplified approach. The finite element model, on the other hand, uses transverse elastoplastic soil springs. As noted previously one obtains the full load p_u from the soil spring only after 0·06 m of the relative transverse displacement between the pipe and the soil. Hence although the full loaded pipe deflects in bending only 0·015 m for $W = 10$ m, the bases of the soil springs must move an additional 0·06 m to obtain the full transverse resistance p_u.

Note that the critical displacements for both the simplified elastic and elastic finite element models in Table II underestimate δ_{cr} for an inelastic pipe shown for example in Figures 5 and 6. This is due to the fact that for the inelastic pipe model, the steel modulus decreases after yielding, and the pipe must undergo larger deformations such that the strain energy in the pipe equals the work done by the distributed soil springs.

The maximum strains in an elastic pipe are due to the combined effects of axial tension (cable behaviour) and flexure (beam behaviour), and can be expressed as

$$\varepsilon_{\text{elastic}} = \begin{cases} \dfrac{\sigma}{E} \pm \dfrac{\pi^2 \delta D}{W^2} & \delta \leqslant \delta_{\text{cr}} \\ \dfrac{\sigma}{E} \pm \dfrac{\pi^2 \delta_{\text{cr}} D}{W^2} & \delta > \delta_{\text{cr}} \end{cases} \tag{11}$$

It can be shown that the σ/E term in equation (11) is approximated by

$$\frac{\sigma}{E} = \begin{cases} \dfrac{\pi\delta}{2} \cdot \sqrt{\dfrac{t_u}{AEW}} & \delta \leqslant \delta_{\text{cr}} \\ \dfrac{\pi\delta_{\text{cr}}}{2} \cdot \sqrt{\dfrac{t_u}{AEW}} & \delta > \delta_{\text{cr}} \end{cases} \tag{12}$$

where A is the pipe cross-sectional area.

The strains estimated by equations (11) and (12) as well as those from the elastic FE model are plotted in Figure 14 as a function of δ for three widths of the PGD zone. As shown in Figure 14, Equations (11) and (12) match reasonably well with the elastic FE results for $W = 30$ and 50 m.

Note that there are differences between Figures 5 and 14. This is due to different modelling assumptions. In Figure 5, an inelastic pipe model is used while in Figure 14, an elastic pipe is assumed. Specifically in the inelastic model, the pipe flexural stiffness is significantly reduced when the axial strain is above the yield strain, while this effect is not present in the model for Figure 14.

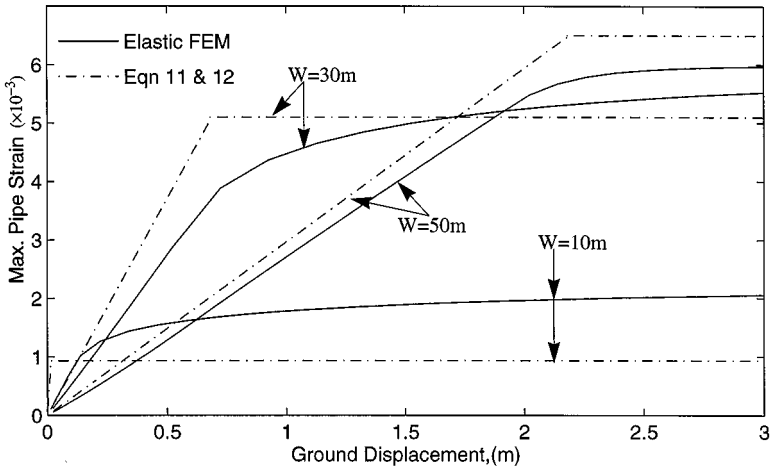

Figure 14. Maximum pipe strain vs. ground displacement

For small widths of the PGD zone (e.g. $W = 10\,\text{m}$) where beam/flexural effects are most predominate, the strain estimated from Equation (11) is less than that from the elastic finite element approach. This is due, in part, to the underestimate of δ_{cr} and $\delta_{cr\text{-bending}}$ mentioned previously. However, as will be noted later, observed values for the width of the PGD zone are typically much larger than 10 m (i.e. $W \geqslant 100\,\text{m}$ typically).

The simplified model (i.e. Equations (11) and (12)) only holds for elastic pipe material cases. For a pipe made of X-52 steel, the yield strain is 0·18 per cent, which corresponds to 0·35 and 0·7 m of ground deformation for $W = 30$ and 50 m, respectively, in Figure 5. Notice that there is a kink in the tensile strain results at those locations. Below the yield strain, the behaviour predicted by the approximate relation matches the inelastic Finite Element results. Above the 'kink', the increase in strain for increase in δ is larger due to the reduced modulus in the Ramberg Osgood pipe material. Never the less, the simplified elastic model does explain the influences of some key parameters. For example, from Equations (11) and (12), it can be shown that the ratio of axial strain to bending strain is an increasing function of width of PGD zone which matches the behaviour shown in Figure 5. For the largest width considered herein (i.e. $W = 50\,\text{m}$), the axial strain is roughly 25 per cent of the bending strain. In addition, the flexural strain in Equation (11) is linearly proportional to diameter D, while the axial strain is inversely proportional to the square root of the diameter. As a result both the tensile and compressive strains, shown in Figure 10 increase with diameter. Similarly the axial strain is proportional to the square root of the peak longitudinal soil resistance t_u while the flexural strain is not a function of this parameter. As a result, both the tensile and compressive strain, as shown in Figure 12, increase mildly with t_u. The effects of changes in the wall thickness t and peak tensile soil resistance are more complex since their influence is related, in large part, to resulting changes in δ_{cr}.

EXPECTED RESPONSE FOR OBSERVED PGD

Although the approximate method described above is strictly applicable for elastic pipe and widths of 30 m or greater, they prove useful for many realistic design situations. By practical situations, we mean observed cases of PGD. For example, Suzuki *et al.*[2] present values for the width W and the amount of movement δ, for transverse PGD observed in the Niigata Japan after the 1964 event. Based on roughly 40 separate sites, the amount of ground movement δ ranged from about 0·3–2·0 m, while the width of the PGD zone W ranged from about 100 m to 600 m.

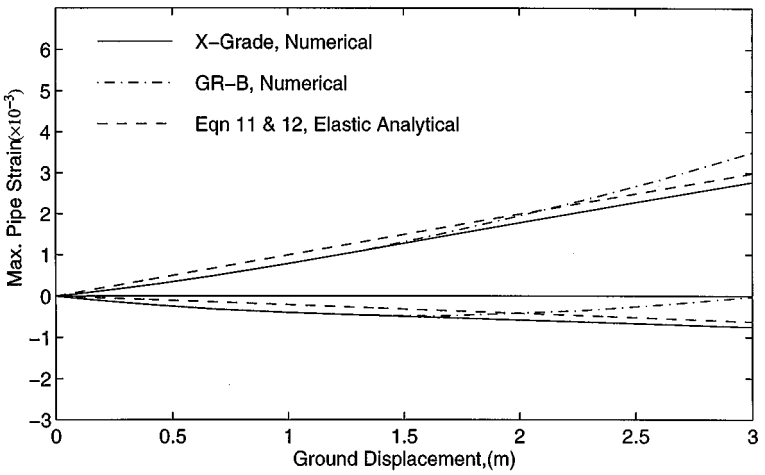

Figure 15. Maximum pipe strain vs. ground displacement for $W = 100$ m

For $W \geqslant 100$ m, steel pipe with $D = 0{\cdot}61$ m, $t = 0{\cdot}0095$ m, the critical ground deformation from Equation (10) is 6·0 m or more, which is much larger than the maximum observed ground displacement of 2·0 m. Also the estimated peak tensile (i.e. combined axial and flexural) strain for $\delta = 2m$ from Equation (11) is less than the yield strain for X-grade steel but slightly above the yield strain for GR-B grade steel. Hence an X-grade pipe behaves elastically and the strain can be estimated by Equations (11) and (12).

The maximum pipe strains are shown in Figure 15 as a function of the ground deformation using both the simplified analytical and numerical models. The finite element results for both X-Grade and GR-B grade steels are identical for δ less than about 1·6 m. At that location there is a kink in the GR-B curve, indicating the onset of inelastic behaviour in that material. Over all the analytical model (i.e. Equations (11) and (12)) results compare favorably with the finite element values. In addition, the comparison among those approaches as well as a case study for a gas pipeline during the 1971 San Fernando earthquake prove the reasonableness of our numerical and analytical results.[8]

The approximate analytical approach does overestimate to some degree the peak tensile strain and underestimates the peak compressive strain. This suggests that the estimated axial strain are somewhat too large. However the differences are relatively small particularly in light of the accuracy of geotechnical predictions for expected value of the spatial extent and ground movement of PGD zones.

CONCLUSION

In this paper, existing approaches and results for buried pipelines subject to spatially distributed transverse PGD are reviewed and compared. New numerical results and analytical approaches are presented which hopefully clarify pipe behaviour when subject to transverse PGD. Although in practice such analyses are often done using commercially available finite element codes, it is felt that the new information presented herein is useful in three aspects. First of all the overall behaviour of the system, specifically the contributions of both flexural (i.e. 'beam-like') and axial (i.e. 'cable-like') effects were highlighted. Secondly the influence of key design parameters such as the wall thickness and the soil resistances were determined. Finally, the influences of modelling parameters, such as the anchor length, on the results were evaluated.

The specific conclusions of this study are as follows:

(a) For small widths of the PGD zone, continuous pipelines behave like a beam and pipe response is controlled by the flexural stiffness. For large widths of the PGD zone, the pipelines also exhibit

'cable-like' behaviour and the pipe response is controlled, in part, by axial forces which are resisted by friction at the pipe–soil interface outside of the PGD zone.

(b) For the pipe considered, flexural strains were larger than axial strain. In addition, peak tensile strain is larger than peak compressive strain.

(c) The assumed anchor length in FE models is an important parameter. Unrealistically, large pipe strain can be developed when the assumed anchor points are too close to the margins of the PGD zone.

(d) Using observed values for the amount and spatial extent of the PGD zone, it is shown that closed form analytical relations developed herein can be used to estimate peak tension and compression strains. This simplified approach can be used for estimating pipe strain when the pipeline is surrounded by a variety of soil types. Specifically, the axial and lateral pipe-soil interaction forces are functions of the soil properties.

ACKNOWLEDGEMENT

The work presented herein was sponsored by the National Center for Earthquake Engineering Research (NCEER). This support is gratefully acknowledged. However, all conclusions are the authors alone and do not necessarily reflect the views of NCEER.

REFERENCES

1. T. D. O'Rourke, 'Critical aspects of soil–pipeline interaction for large ground deformation', *Proc. 1st Japan–U.S. Workshop on Liquefaction, Large Ground Deformation and Their Effects on Lifeline Facilities*, November 1988, pp. 118–126.
2. N. Suzuki, T. Kobayashi, H. Nakane and M. Ishikawa, 'Modelling of permanent ground deformation for buried pipelines', *Proc. 2nd U.S.–Japan Workshop on Liquefaction, Large Ground Deformation and Their Effects on Lifelines*, 1989, pp. 413–425.
3. M. J. O'Rourke, 'Approximate analysis procedures for permanent ground deformation effects on buried pipelines', *Proc. 2nd U.S.–Japan Workshop on Liquefaction, Large Ground Deformation and Their Effects on Lifelines*, 1989, pp. 336–347.
4. M. J. O'Rourke, X. Liu, R. Flores-Berrones, 'Steel pipe wrinkling due to longitudinal permanent ground deformation', *J Transportation Engng.* **121**, 443–451 (1995).
5. T. D. O'Rourke, M. J. O'Rourke, 'Pipeline response to permanent ground deformation: a benchmark case', *Proc. 4th U.S. Conf. on Lifeline Earthquake Engineering*, TCLEE, ASCE, San Francisco, California, August 1995, pp. 288–295.
6. N. Suzuki, O. Arata and I. Suzuki, 'Subject to liquefaction-induced permanent ground displacement', *Proc. 1st Japan–U.S. Workshop on Liquefaction, Large Ground Deformation and Their Effects on Lifeline Facilities*, November 1988, pp. 155–162.
7. ASCE, *Guidelines for the Seismic Design of Oil and Gas Pipeline Systems*, Committee on Gas and Liquid Fuel Lifeline, ASCE, 1984.
8. X. Liu, Response of buried continuous pipelines subject to earthquake effects, *Ph.D. Dissertation*, Department of Civil Engineering, Rensselear Polytechnic Institute, December, 1996, 143p.

